



Autotaxin Production of Lysophosphatidic Acid Mediates Allergic Asthmatic Inflammation

Gye Young Park^{1,2*}, Yong Gyu Lee^{1*}, Evgeny Berdyshev^{1,3*}, Sharmilee Nyenhuis^{1,2}, Jian Du⁴, Panfeng Fu^{3,5}, Irina A. Gorshkova^{1,3}, Yongchao Li⁶, Sangwoon Chung¹, Manjula Karpurapu¹, Jing Deng¹, Ravi Ranjan¹, Lei Xiao¹, H. Ari Jaffe^{1,2}, Susan J. Corbridge⁷, Elizabeth A. B. Kelly⁸, Nizar N. Jarjour⁸, Jerold Chun⁹, Glenn D. Prestwich¹⁰, Eleanna Kaffe¹¹, Ioanna Ninou¹¹, Vassilis Aidinis¹¹, Andrew J. Morris¹², Susan S. Smyth¹², Steven J. Ackerman^{1,4,†}, Viswanathan Natarajan^{1,3,5,†}, and John W. Christman^{2,13,†}

¹Section of Pulmonary, Critical Care, Sleep, and Allergy, Department of Medicine, ³Institute for Personalized Respiratory Medicine, ⁴Department of Biochemistry and Molecular Genetics, ⁵Department of Pharmacology, College of Medicine, ⁶Department of Medicinal Chemistry, College of Pharmacy, and ⁷Department of Biobehavioral Health Science, College of Nursing, University of Illinois, Chicago, Illinois; ²Jesse Brown Veterans Affairs Medical Center, Chicago, Illinois; ⁸Allergy, Pulmonary, and Critical Care Division, Department of Medicine, University of Wisconsin, Madison, Wisconsin; ⁹Dorris Neuroscience Center, The Scripps Research Institute, La Jolla, California; ¹⁰Department of Medicinal Chemistry, the University of Utah, Salt Lake City, Utah; ¹¹Institute for Immunology, Athens, Greece; ¹²Department of Medicine, University of Kentucky College of Medicine, Lexington, Kentucky; and ¹³Section of Pulmonary, Allergy, Critical Care, and Sleep Medicine, the Ohio State University, Columbus, Ohio

Rationale: Bioactive lipid mediators, derived from membrane lipid precursors, are released into the airway and airspace where they bind high-affinity cognate receptors and may mediate asthma pathogenesis. Lysophosphatidic acid (LPA), a bioactive lipid mediator generated by the enzymatic activity of extracellular autotaxin (ATX), binds LPA receptors, resulting in an array of biological actions on cell proliferation, migration, survival, differentiation, and motility, and therefore could mediate asthma pathogenesis.

(Received in original form June 4, 2013; accepted in final form August 15, 2013)

* These authors contributed equally to this work.

† These authors contributed equally as senior authors.

Supported in part by the National Institutes of Health (NIH) grants R01 HL075557 and HL103643 (J.W.C.) and HL P01 58064 and 98050 (V.N.) and a pilot grant from the University of Illinois Center for Clinical and Translational Science (UIC-CCTS), NIH-National Center for Advancing Translational Science (NCATS) grant UL1TR000050 (S.J.A.), and a Department of Veterans Affairs merit review grant (J.W.C.). G.Y.P. was supported by NIH grant T32 HL082547. The SBP-AG protocol at the University of Wisconsin was supported by P01 HL088594, HL056396, M01 RR03186, and UL1 RR025011. Statistical analysis was supported by UIC-CCTS (NIH-NCATS, UL1TR000050).

Author Contributions: G.Y.P. performed SBP-AG protocol, designed animal experiments, analyzed data, generated figures, and drafted and edited the manuscript. Y.G.L. performed the mouse and cellular experiments, generated figures, and edited the manuscript. E.B. directs the lipidomics laboratory, performed LC/MS/MS and analyzed the data, and edited manuscript. S.N. wrote and maintained the SBP-AG IRB and IND protocol, led SBP-AG patient recruitment efforts, and edited the manuscript. J. Du performed the SBP-AG BAL and blood inflammatory cell purification protocols. P.F. performed ATX Western blots and assisted G.Y.P. in animal experiments. I.A.G. and Y.L. assisted with the LC/MS/MS measurement of LPA. S.C., M.K., R.R., J. Deng, and L.X. assisted with the DRA triple-allergen animal model and cytokine measurement. H.A.J. and S.J.C. assisted with SBP-AG IRB and IND protocols and performance of bronchoscopy. N.N.J. and E.A.B.K. supervised the SBP-AG protocol and provided BAL fluids and plasma from the Wisconsin cohort. J.C. supplied LPA₂^{-/-} mice breeding pair. G.D.P. supplied the ATX inhibitor, GWJ-23. V.A., E.K., and I.N. were involved in discussions related to animal dosage. A.J.M. and S.S.S. provided breeding pairs of ATX-Tg and ATX^{+/-} mice. S.J.A. managed the inflammatory cell purification core lab for the SBP-AG protocol, designed experiments, interpreted data, coordinated regular scientific research meetings for the project, and edited the manuscript. V.N. conceptualized the study, designed mouse experiments, interpreted data, provided genetically modified mice, and wrote part of and edited the manuscript. J.W.C. obtained the SBP-AG IRB and IND approval, supervised mouse experiments and performance of the human SBP-AG protocol, designed experiments, interpreted and analyzed data, and edited the manuscript. All authors contributed to data discussion and review of the manuscript.

Correspondence and requests for reprints should be addressed to John W. Christman, M.D., The Ohio State University Wexner Medical Center, 201 Davis Heart and Lung Research Institute, 473 West 12th Avenue, Columbus, OH 43210. E-mail: john.christman@osumc.edu

This article has an online supplement, which is accessible from this issue's table of contents at www.atsjournals.org

Am J Respir Crit Care Med Vol 188, Iss. 8, pp 928–940, Oct 15, 2013

Copyright © 2013 by the American Thoracic Society

Originally Published in Press as DOI: 10.1164/rccm.201306-1014OC on September 19, 2013
Internet address: www.atsjournals.org

AT A GLANCE COMMENTARY

Scientific Knowledge on the Subject

Lysophosphatidic acid (LPA) is a bioactive lipid mediator with multiple functions, particularly as an inducer of cell proliferation, migration, and survival. Although most studies to date have focused on the role of LPA in diseases of blood vessels, cancer, and idiopathic pulmonary fibrosis, there is a lack of studies on how LPA participates in allergic inflammation, particularly in the lung in asthma.

What This Study Adds to the Field

The enzyme autotaxin (ATX) and two of its LPA products, LPA 22:5 and LPA 22:6, are markedly and selectively increased in the bronchoalveolar lavage fluid of human patients with asthma in response to airway allergen challenge. The ATX/LPA pathway also plays a critical role in the development of allergic lung inflammation in a murine allergic asthma model. The results of this study suggest that interventions targeting the ATX/LPA pathway could lead to the development of a new class of therapy for human asthma.

Objectives: To define a role for the ATX-LPA pathway in human asthma pathogenesis and a murine model of allergic lung inflammation.

Methods: We investigated the profiles of LPA molecular species and the level of ATX exoenzyme in bronchoalveolar lavage fluids of human patients with asthma subjected to subsegmental bronchoprovocation with allergen. We interrogated the role of the ATX-LPA pathway in allergic lung inflammation using a murine allergic asthma model in ATX-LPA pathway-specific genetically modified mice.

Measurements and Main Results: Subsegmental bronchoprovocation with allergen in patients with mild asthma resulted in a remarkable increase in bronchoalveolar lavage fluid levels of LPA enriched in polyunsaturated 22:5 and 22:6 fatty acids in association with increased concentrations of ATX protein. Using a triple-allergen mouse asthma model, we showed that ATX-overexpressing transgenic mice had a more severe asthmatic phenotype, whereas blocking ATX activity and knockdown of the LPA₂ receptor in mice produced a marked attenuation of Th2 cytokines and allergic lung inflammation.

Conclusions: The ATX-LPA pathway plays a critical role in the pathogenesis of asthma. These preclinical data indicate that targeting the ATX-LPA pathway could be an effective antiasthma treatment strategy.

Keywords: asthma; lysophosphatidic acid; autotaxin; allergic airway inflammation

Lysophosphatidic acid (LPA) is a naturally occurring biologically active lipid that is generated from lysophosphatidylcholine (LPC) by the extracellular enzyme, autotaxin (ATX), also known as lysophospholipase D (lysoPLD). ATX is present in plasma, saliva, follicular fluid, and malignant effusions (1, 2). Through engagement with distinct high-affinity cell-surface G-protein-coupled receptors, LPA exhibits a wide range of effects on a variety of cell types, including bronchial epithelium, smooth muscle cells, fibroblasts, and lymphocytes (3–5). LPA augments cytokine synthesis and chemotaxis in lymphocytes (6–9), induces contractility and proliferation of airway smooth muscle cells (10), and modulates inflammatory signaling in bronchial epithelial cells (10–12), suggesting a possible role in the molecular pathogenesis of asthma. In this regard, LPA has been shown to increase intracellular Ca^{2+} and chemotaxis of Th2 T cells (13), augment IL-13 gene expression and secretion by activated T cells, and enhance transcriptional activity of the IL-13 promoter in Th2 cells (9). Thus, LPA could play a role in Th2 chemotaxis and cytokine release in allergen-induced asthmatic airway inflammation and remodeling. *In vitro*, LPA has chemotactic activity for inflammatory cells, such as eosinophils, and stimulates eosinophil superoxide production, increases intracellular Ca^{2+} , and induces actin polymerization (14). *In vivo*, LPA aerosol inhalation in the guinea pig was found to induce eosinophil and neutrophil recruitment into the airspaces and induced airways hyperreactivity (6). Increased LPA levels and LPA 22:6 molecular species have been reported in bronchoalveolar lavage (BAL) fluids after segmental allergen challenge of patients with asthma (15). LPA levels were increased in the airways of patients with idiopathic pulmonary fibrosis and in BAL fluids after bleomycin-induced lung injury of mouse model, and mice lacking the LPA_1 receptor were markedly protected from fibrosis and mortality (16). To our knowledge, no other studies to date have directly addressed the roles of ATX, LPA, and its cognate receptors in allergic airway inflammation and the asthmatic diathesis in human subjects.

In the current study, we have interrogated the ATX/LPA axis in patients with mild asthma subjected to subsegmental bronchoprovocation with allergen (SBP-AG) to induce localized allergic lung inflammation, and in a triple-allergen—house dust mite, ragweed, *Aspergillus* sp. (DRA)—mouse model of allergic asthma in studies using ATX overexpressing transgenic, heterozygous $\text{ATX}^{-/+}$ deficient (knockout) mice combined with pharmacologic inhibition of ATX enzymatic activity, and LPA_2 receptor knockout mice. Our findings in both human asthmatic SBP-AG subjects and mouse allergic asthma models show that LPA levels are substantially increased in the airspaces in response to allergen challenge, that signature polyunsaturated LPA species (LPA 22:5 and 22:6) comprise more than 50% of the released LPA, and that blocking ATX expression/enzyme activity and LPA receptor expression in the mouse allergic asthma model substantially abrogates airway inflammation in terms of both inflammatory cell recruitment and expression of Th2 cytokines. These findings support a role for ATX, its unique polyunsaturated LPA products, and their receptors in the pathogenesis of asthma, suggesting novel therapeutic targets for asthma intervention.

METHODS

SBP-AG Bronchoscopy Protocol

This protocol was approved by the Institutional Review Board of the University of Illinois (Chicago, IL), and an investigational new drug was obtained from the U.S. Food and Drug Administration for

bronchoscopic administration of allergens to volunteers. Subjects underwent screening for inclusion and exclusion criteria that included skin prick testing to house dust mite, short ragweed, and cockroach allergens and spirometry with bronchodilator reversibility and/or methacholine challenge. Subjects taking asthma-controlling medications were excluded. To obtain the prechallenge bronchial sample, BAL was performed at a subsegmental bronchus before allergen challenge. Subsegmental bronchoprovocation with the identified allergen (SBP-AG) was performed in a different subsegment. A starting dose of 10-fold greater than the previously defined skin endpoint titration dose in bioequivalent allergen units (BAU) or weight/volume (wt/vol) of allergen was administered. If no significant airway edema was noted after 10 minutes, the challenge dose of allergen (i.e., 100-fold greater than the previously defined skin endpoint titration dose) was administered to the subsegment. The maximum challenge dose for SBP-AG was 5 mL of a 100 BAU/mL or 1:2,000 wt/vol concentration of allergen. At 48 hours after the initial bronchoscopy, BALs from three different sites were obtained from the unchallenged segment contralateral to the challenge site (contralateral site), the unchallenged segment adjacent to the challenged lobe (adjacent site), as well as the challenged segment of the challenged lobe (experimental site) (*see* Figure E1 in the online supplement). Additional detail on the methods for the SBP-AG protocol is provided in the online supplement.

Mice

All of the mice were bred and housed in a specific pathogen-free barrier facility maintained by the University of Illinois at Chicago, Biologic Resources Laboratory. All experiments involving mice were conducted with protocols approved by the Institutional Animal Care and Use Committee of the University of Illinois (Chicago, IL). Adult male, 8- to 10-week-old mice with an average weight of 20 to 25 g were used for the experiments. The breeding pairs of ATX-Tg and ATX heterozygous ($\text{ATX}^{+/-}$) mice on the FVB background, provided by Dr. Susan Smyth (University of Kentucky), were successfully bred at the University of Illinois at Chicago (UIC) animal facility (17). $\text{LPA}_2^{-/-}$ mice were provided by Dr. Chun (The Scripps Research Institute, La Jolla, CA) (18).

Lung Tissue Preparation

Mouse lung tissue was prepared using pressurized low-melting agarose. Briefly, 0.5% wt/vol low-melting-point agarose was boiled at 60°C and then kept at 42°C in water bath. After tracheostomy was performed, the 0.5% melted agarose was infused through the tracheostomy tube from height of 28 cm H_2O to pressurize equally over lung fields. The tracheostomy tube was tied and lung tissue was put into a formalin container that was refrigerated overnight to facilitate solidification and fixation. Additional detail on the method for Western blot and immunohistochemistry is provided in the online supplement.

DRA Triple-Allergen Asthma Model

We used the published triple-allergen (DRA)-induced allergic mouse asthma model with minor modifications (19) to recapitulate the pathophysiologic features of SBP-AG of human patients with asthma. Additional detail on the method for the DRA triple-allergen asthma model is provided in the online supplement and Figure E2.

Morphometric Analysis and Digital Pathology

We used the Genie System (Aperio Technologies, Vista, CA), a tool for automated classification of tissue in whole slide images. Additional detail on this method is provided in the online supplement.

Liquid Chromatography with Tandem Mass Spectrometry

Levels of total LPA and its molecular species were determined as described previously (15, 20), with minor modifications. Additional detail on the method for liquid chromatography with tandem mass spectrometry (LC/MS/MS) is provided in the online supplement.

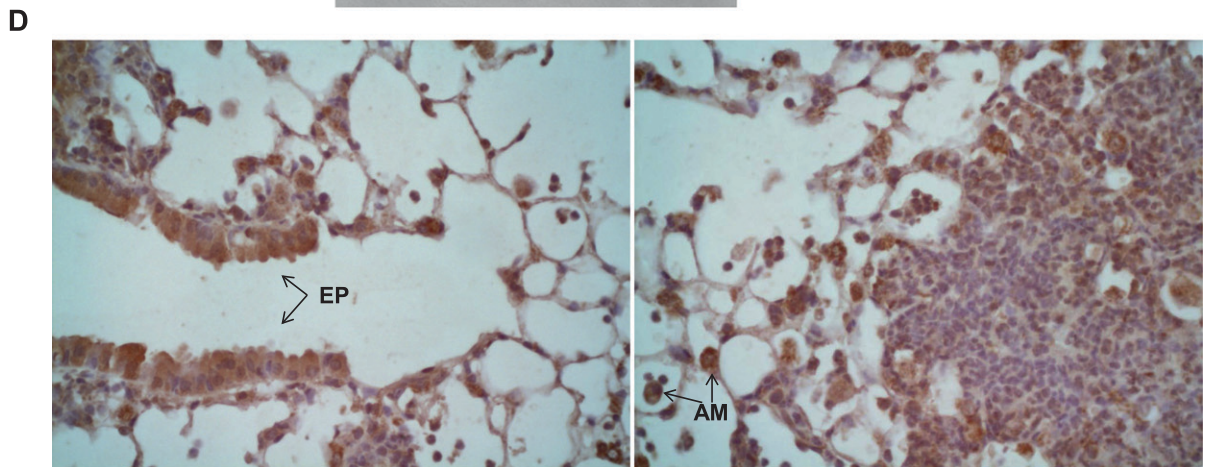
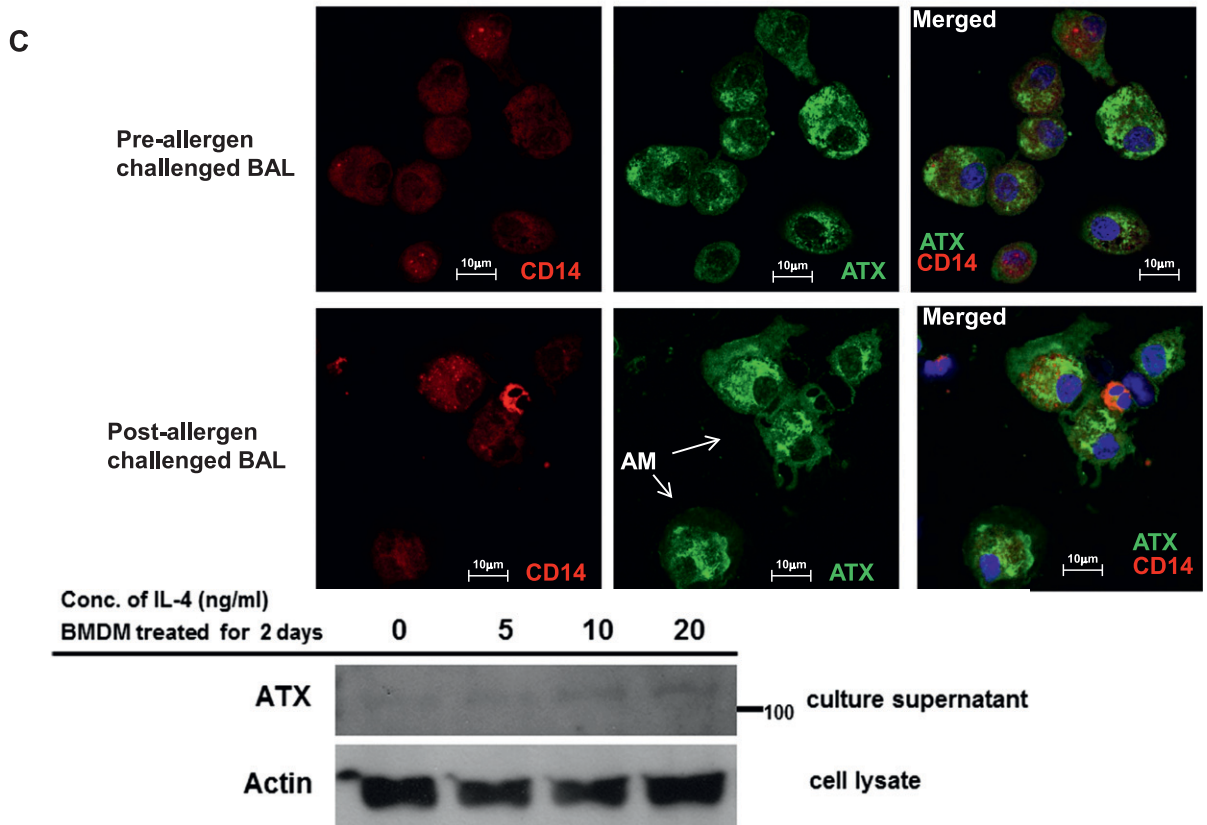
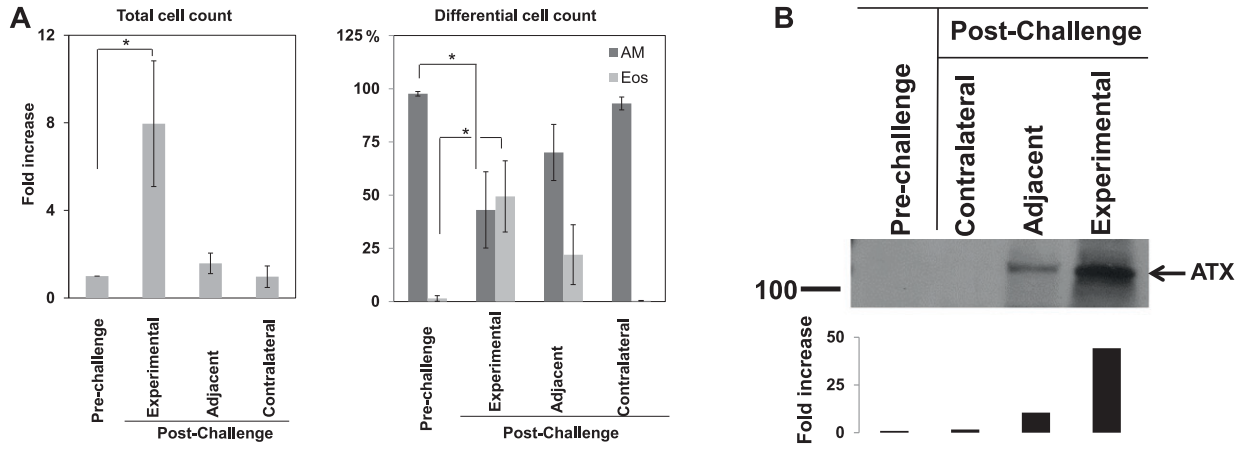


Figure 1. (A) Total cell and differential counts of bronchoalveolar lavage (BAL) fluid recovered from patients with mild asthma enrolled in the subsegmental bronchoprovocation with allergen (SBP-AG) protocol. The total cell count increased approximately eightfold in the BAL fluid from the allergen-challenged subsegment and consisted primarily of eosinophils (Eos) and alveolar macrophages (AM). There was only a mild increase in the eosinophil count in the adjacent segment and no increase in the contralateral segment, indicating that the allergic reaction was confined to the experimental site, with minimal spillover to adjacent segments. $n = 4$. * $P < 0.05$. (B) Western immunoblot for autotaxin (ATX) in BAL fluid samples obtained pre- and post-allergen challenge in the SBP-AG protocol. The BAL fluids were obtained from patients with mild asthma before and after allergen challenge as described in Figure E1. BAL fluid (40 μ l/lane) from each of the different lung subsegments was analyzed. The strongest band was ~ 110 kD, corresponding to the size of ATX as reported in the literature (3). The 110-kD bands were completely abolished by preabsorption of the anti-ATX antibody with an ATX-specific peptide (Figure E3). Analyses of BAL fluids from two additional SBP-AG subjects provided identical results. The signal density of immunoblot was measured using Image J software. (C) Immunofluorescent staining for ATX in BAL cells recovered from an SBP-AG protocol subject pre- and post-allergen challenge. Cytospin slides of BAL cells from an SBP-AG asthma subject were prepared from the allergen-challenged subsegment before and after allergen challenge and stained by immunofluorescence for CD14 and ATX. Anti-CD14 (pink) was used a biomarker for AM. The anti-ATX antibody was conjugated with green fluorescent protein (green). In the *bottom panel*, murine bone marrow-derived macrophages (BMDM) were treated with various concentrations of IL-4 (0–20 ng/ml) for 48 hours, and the culture supernatants were analyzed by Western blotting for ATX; a dose–response relationship was demonstrated for the IL-4-induced secretion of ATX by BMDM. The entire image of this immunoblot is provided in the online supplement (Figure E4). (D) Immunohistochemistry for ATX expression in allergic lung inflammation induced by the triple-allergen (house dust mite, ragweed, *Aspergillus* sp.) mouse model. ATX was highly expressed in airway epithelial cells in the distal airway, mostly on the luminal side, as well as by AM, whereas expression by endothelial cells, eosinophils, and type 1 pneumocytes was significantly lower or minimal. Additional images are provided in the online supplement (Figures E5 and E6). EP = bronchial epithelial cells.

Statistical Analysis

Statistical analyses were performed independently by a professional statistician at the Center for Clinical and Translation Science, Design and Analysis Core at UIC. In brief, normality was examined for all data using Kolmogorov-Smirnov test and Q-Q plots. For normal distributed data, the two-sample *t* test was used for two-group comparisons with equal variance or unequal variance assumptions. For nonnormal distributed data, a nonparametric method (signed rank test) was used for comparisons of two paired samples. All analyses were conducted using the SAS statistical package (version 9.2, SAS Institute, Cary, NC).

RESULTS

Increased ATX Protein Is Present in BAL Fluid of Patients with Asthma after Allergen Challenge and in Lung Tissue of Mice Subjected to a Triple-Allergen Model of Asthma

Volunteers with mild asthma were recruited and screened for the study using allergen skin testing to identify the allergen as well as spirometry with a bronchodilator response or a methacholine challenge test to confirm asthma. Subjects meeting inclusion criteria underwent SBP-AG; BAL was performed before allergen challenge and at 48 hours after allergen challenge (Figure E1). As demonstrated, allergen challenge resulted in pronounced eosinophilic allergic lung inflammation in a localized fashion (Figure 1A). ATX protein expression was determined by Western blotting of BAL fluid obtained before allergen challenge and from three different locations after allergen challenge using the SBP-AG protocol. A remarkable increase in ATX level was documented in the allergen-challenged site compared with the prechallenge or contralateral post-challenge sites, with a significantly lower level in the subsegment adjacent to the allergen-challenged site (Figure 1B). Because this was unexpected, the specificity of the ATX immunoblot was confirmed by using an antibody-neutralizing peptide (Figure E3). Before allergen challenge, ATX was observed in the cytoplasm of alveolar macrophages and shifted to a perinuclear localization in response to allergen challenge (Figure 1C, *upper panel*). Although it was not possible to culture a sufficient number of human alveolar macrophages, bone marrow-derived murine macrophages were treated with IL-4 and found to secrete ATX into the culture supernatant (Figure 1C, *lower panel*; Figure E4).

We subjected mice to sensitization and challenge with a combination of house dust mite, ragweed, and *Aspergillus* allergen (DRA), as previously described, with minor modifications (19).

DRA included two of the major allergens used for the human SBP-AG protocol. This triple-allergen DRA model produced abundant eosinophilic allergic lung inflammation (Figure E2). In this model, ATX protein was detected by immunostaining in lung tissue, especially in terminal bronchial epithelial cells and alveolar macrophages, whereas endothelial cells, eosinophils, and type 1 pneumocytes showed minimal ATX staining (Figure 1D and Figures E5–E7).

Polyunsaturated LPA 22:5 and 22:6 Are the Major LPA Molecular Species Present in BAL Fluid of Allergen-challenged Patients with Asthma

We next measured the enzymatic product of ATX, LPA, in the UIC SBP-AG discovery cohort ($n = 4$) by using LC/MS/MS (Figure 2A). Total LPA levels in BAL fluids were increased by allergen challenge in patients with mild asthma, mainly due to the elevation of LPA 22:5 and 22:6, with individual increases ranging from 2- to 100-fold (Figure 2B). Interestingly, LPA 22:5 was increased only in the allergen-challenged lung segment, with very little spillage into adjacent pulmonary subsegments (Figures E8 and E9). We also analyzed an independent verification cohort of patients with mild asthma who were subjected to the SBP-AG protocol at the University of Wisconsin (Wisconsin cohort). Twenty-one additional paired pre- and post-allergen-challenge BAL fluids and nine paired plasma samples were analyzed. Before allergen challenge, saturated LPA 16:0 and LPA 18:0 were the predominant species in BAL fluid of the patients with mild asthma (Figure 2C, *solid bar*). In response to allergen challenge, there was a major increase in polyunsaturated LPA 22:5 and, to a lesser degree, LPA 22:6 (Figure 2C). In the Wisconsin cohort, LPA 22:5 and LPA 22:6 were significantly increased by 11- and 7-fold, respectively, in response to allergen challenge (Figure 2D). However, the levels of saturated LPA 16:0 and LPA 18:0 were not affected by the allergen challenge (Figure 2E and Figure E10). In the Wisconsin cohort, there was a slight but statistically significant elevation of total plasma LPA level (Figure 2F), which was attributed to a small increase in saturated LPA 16:0 and LPA 18:0, in contrast to the pattern seen in BAL fluids (Figures 2G and 2H). These data indicate that polyunsaturated LPA 22:5 and LPA 22:6 are produced within the lavageable airspaces and are not due simply to extravasation from plasma.

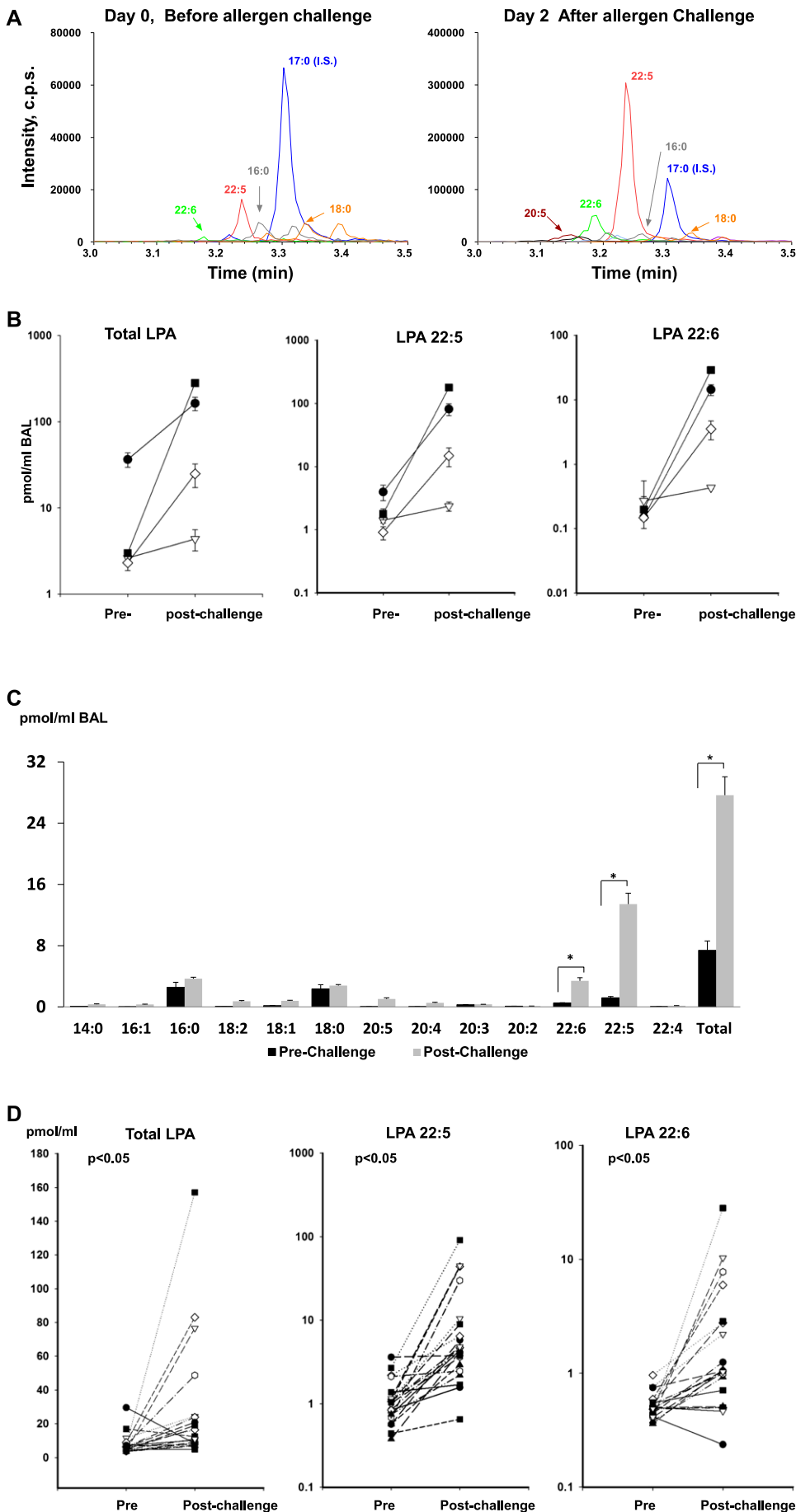


Figure 2. (A) Representative figure of the lysophosphatidic acid (LPA) molecular species identified by liquid chromatography with tandem mass spectrometry (LC/MS/MS) in the bronchoalveolar lavage (BAL) fluid of a subject with mild asthma enrolled in the subsegmental bronchoprovocation with allergen (SBP-AG) protocol before and after allergen challenge. There was a significant increase in polyunsaturated LPA 22:5, and to a lesser degree polyunsaturated LPA 22:6, at the allergen-challenged experimental site. (B) Total LPA, LPA 22:5, and LPA 22:6 in BAL fluid pre- and post-allergen challenge in the University of Illinois at Chicago (UIC) discovery cohort (n = 4). LPA levels were quantified in BAL fluid from the allergen-challenged lung subsegment; the standard error for each value represents the variation in the measurement among the four separate aliquots of the BAL fluid return. LPA 22:5 and LPA 22:6 were elevated by allergen challenge ranging from 2- to 100-fold increases, contributing to the overall increase in total LPA. (C) Profiles of the various LPA molecular species in the BAL fluids of patients with mild asthma subjected to the SBP-AG protocol in the Wisconsin verification cohort (n = 21). LPA levels were measured by LC/MS/MS as described in METHODS. Changes in the LPA level pre- and post-allergen challenge were analyzed statistically using the paired *t* test as described in METHODS. **P* < 0.05. (D) Levels of total and polyunsaturated LPA molecular species, LPA 22:5 and LPA 22:6, in the BAL fluid of subjects with mild asthma induced by the SBP-AG protocol in the Wisconsin cohort. LPA levels pre- and post-allergen challenge were compared statistically using the paired *t* test as described in METHODS. (E) Levels of saturated LPA molecular species, LPA 16:0 and LPA 18:0, in the BAL fluid of subjects with mild asthma undergoing the SBP-AG protocol in the Wisconsin cohort. The pre- and post-allergen challenge LPA levels were compared statistically using the paired *t* test as described in METHODS. (F) Profiles of LPA molecular species in the plasma of patients with mild asthma induced by the SBP-AG protocol in the Wisconsin cohort (n = 9). LPA levels were measured by LC/MS/MS as described in METHODS. LPA levels pre- and post-allergen challenge were compared using the paired *t* test as described in METHODS. **P* < 0.05. (G) Levels of total and saturated LPA molecular species, LPA 16:0 and LPA 18:0, in the plasma of subjects with mild asthma induced by the SBP-AG protocol in the Wisconsin cohort. The pre- and post-allergen challenge LPA levels were compared using the paired *t* test as described in METHODS. (H) Levels of the polyunsaturated LPA molecular species, LPA 22:5 and LPA 22:6, in the plasma of subjects with mild asthma induced by the SBP-AG protocol in the Wisconsin cohort. The pre- and post-allergen challenge LPA levels were compared statistically using the paired *t* test as described in METHODS.

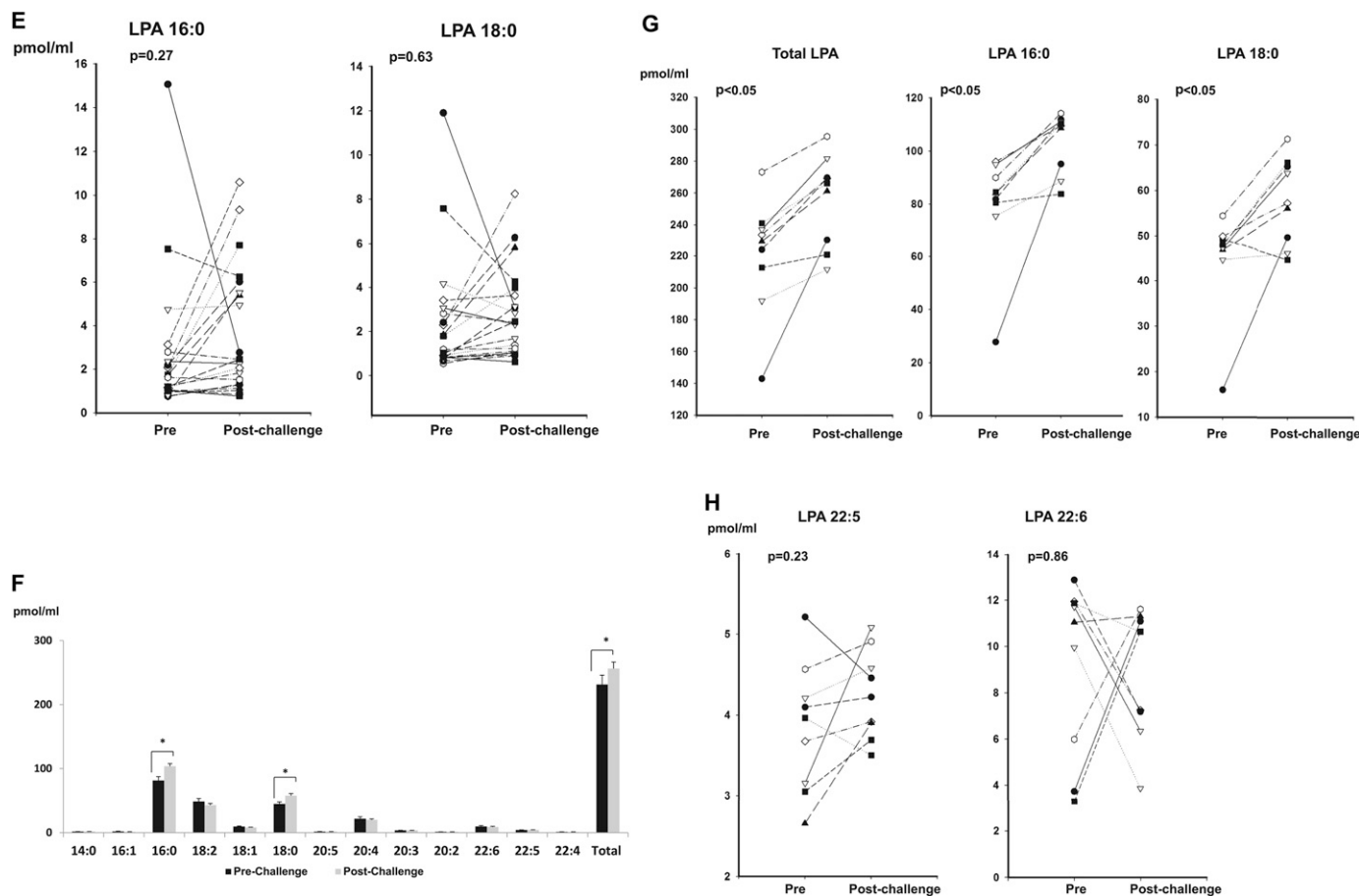


Figure 2. (continued).

Overexpression of ATX Accentuates Allergic Lung Inflammation

As a strong association between allergen challenge, ATX protein production, and generation of polyunsaturated LPA 22:5 and LPA 22:6 in human BAL fluids from allergen-challenged patients with asthma was observed, we next investigated the role of the ATX/LPA axis in the pathogenesis of asthma by using genetically modified mice. First, we compared transgenic mice that overexpressed ATX (ATX-Tg) to wild-type (WT) mice (WT-FVB) of the same background that were subjected to the triple-allergen DRA asthma model. Some polyunsaturated LPA 22:5 was present in BAL fluid in the control mice (Figure E11), and DRA challenge increased the level of LPA 22:5 in BAL fluid compared with sham (phosphate-buffered saline)-challenged mice (Figure 3A and Figure E11). Compared with WT mice, ATX-Tg mice had more inflammatory cells, mostly eosinophils (Figure 3B), but there was no difference in the percentage differential cell counts (Figure E12). Total serum IgE was elevated in response to DRA sensitization equally in both groups of mice (Figure 3C). In the DRA model, the levels of IL-4 and IL-5 in lung homogenates and BAL fluids were significantly greater in ATX-Tg mice (Figures 3D and 3E) compared with WT mice (WT-FVB), whereas IFN- γ showed no change between the two groups (data not shown). We analyzed the severity of allergic lung inflammation by using automated digital morphometric analyses of cross-sections of the entire lung field. ATX-Tg mice had a greater degree of lung inflammation compared with WT mice when subjected to DRA challenge (Figure 3F and Figure E13). ATX-Tg mice also

showed a greater degree of goblet cell metaplasia than WT mice in response to allergen (Figure 3G and Figure E14).

Blocking the ATX/LPA Axis Attenuates Allergic Lung Inflammation

We next determined if blocking the ATX-LPA pathway attenuates allergic lung inflammation. LPA receptor 2 (LPA₂) has been shown to be expressed in the lung tissue and in many cell types (21), and preliminary studies showed that LPA₂ mRNA was highly expressed by eosinophils (data not shown). Therefore, we used LPA₂ knock-out mice (LPA₂^{-/-}) that have defective LPA₂ receptor signaling (18). Our data showed that DRA-sensitized and -challenged LPA₂^{-/-} mice had fewer inflammatory cells in BAL fluid (Figure 4A) and attenuated levels of IL-4 and IL-5 in lung tissue and BAL fluid, compared with WT mice with the same genetic background (WT-129SV) (Figures 4B and 4C), whereas IFN- γ showed no change between the two groups (data not shown). Surprisingly, LPA22:5 levels in BAL fluids of LPA₂^{-/-} mice showed a blunted response, suggesting a possible link between the LPA₂ receptor and LPA 22:5 production (Figure 4D). Quantification of lung pathology also showed a lesser degree of inflammation with the DRA model in LPA₂^{-/-} mice (Figure 4E and Figure E15).

Pharmacologic Inhibition of ATX Enzymatic Activity Reduces the Severity of the Murine Asthmatic Phenotype

Next, we determined whether inhibiting ATX affects allergic lung inflammation. Because total knockdown of ATX is embryonic

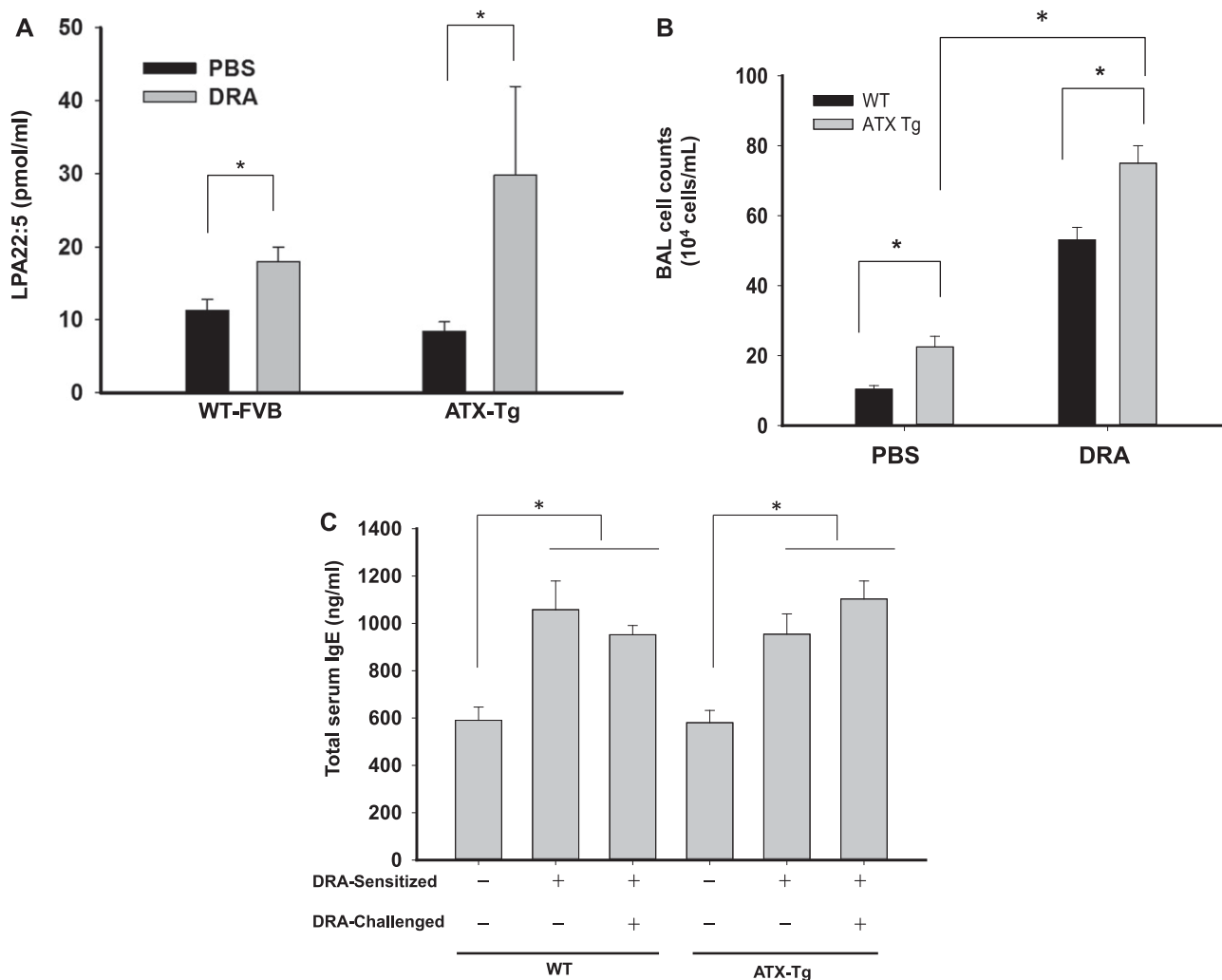


Figure 3. (A) The level of lysophosphatidic acid (LPA) 22:5 was analyzed in bronchoalveolar lavage (BAL) fluids from autotaxin (ATX)-overexpressing transgenic mice (ATX-Tg) and wild-type (WT)-FVB mice induced by the house dust mite, ragweed, *Aspergillus* sp. (DRA) triple-allergen model. LPA levels were measured by liquid chromatography with tandem mass spectrometry as described in METHODS. $*P < 0.05$; $n = 4$. (B) Total cell counts in BAL fluid of ATX-Tg mice had higher number of BAL cells before and after allergen challenge, compared with WT mice of the same background. $*P < 0.05$. (C) Total serum IgE concentrations in WT versus ATX-Tg mice as induced by the DRA triple-allergen model. Total serum IgE levels were measured by ELISA as described in the online supplement. $*P < 0.05$. (D) Concentration of IL-4 in lung homogenates and BAL fluids of ATX-Tg versus WT-FVB mice induced by the DRA triple-allergen model. Experiments were done at least twice with similar results. $n \geq 5$ mice per group. $*P < 0.05$. (E) Concentration of IL-5 in lung homogenates and BAL fluids of ATX-Tg and WT-FVB mice induced by the DRA triple-allergen model. Experiments were performed at least twice with similar results. $n \geq 5$ mice per group. $*P < 0.05$. (F) The pathologic severity of allergic lung inflammation in ATX-Tg versus WT-FVB mice induced by the DRA triple-allergen model. Total lung inflammation was quantified using digital morphometry software systems as described in METHODS. Whole lung fields were scanned and analyzed to classify regional involvement of inflammation in a blinded fashion. The numeric values correspond to the percentage of the regional area of lung inflammation. The analysis was repeated at least twice with similar results. The color codes represent the following: green = inflammation, blue = alveolar space, yellow = structural tissue, and pink = void area. (G) Quantitation of goblet cell metaplasia in ATX-Tg versus WT-FVB mice induced by the DRA triple-allergen model. Using the digital morphometric software system described in METHODS, bronchial epithelial cells were automatically identified. The presence of periodic acid Schiff (PAS) staining was assessed using the same threshold setting for the whole lung field. The left figures show the raw PAS staining, the middle figures show the identification of individual bronchial epithelial cells, and the right figures identify the PAS-positive goblet cells using digital signal threshold as described in METHODS. The numeric values represent the percentage of PAS-positive cells of total bronchial epithelial cells. The analysis was repeated at least twice with similar results. PBS = phosphate-buffered saline.

lethal, we used ATX^{+/-} heterozygous (ATX-het) mice that express ~50% less ATX than their WT counterparts (17). We also used a selective pharmacological inhibitor, GWJ-23 (Figure E16), to block the remaining ATX enzymatic activity (22, 23) following the protocol described in Figure 5A. Compared with WT mice, the ATX-het mice had lower levels of IL-4 and IL-5 in BAL fluids and lung tissues induced in the DRA model, which were further

suppressed by pretreatment with the ATX inhibitor (Figures 5B and 5C). The ATX inhibitor, GWJ-23, blocked choline release from LPC16:0 with a K_i (nM) of 73 and inhibitory concentration 50% (nM) of 140 (Figure E16) *in vitro*. *In vivo*, plasma LPA levels were significantly diminished at 0.5, 1, 2, 4, 8, and 16 hours post GWJ-23 administration comparable to LPA levels of vehicle controls with a maximum concentration of 40 μ M at maximum

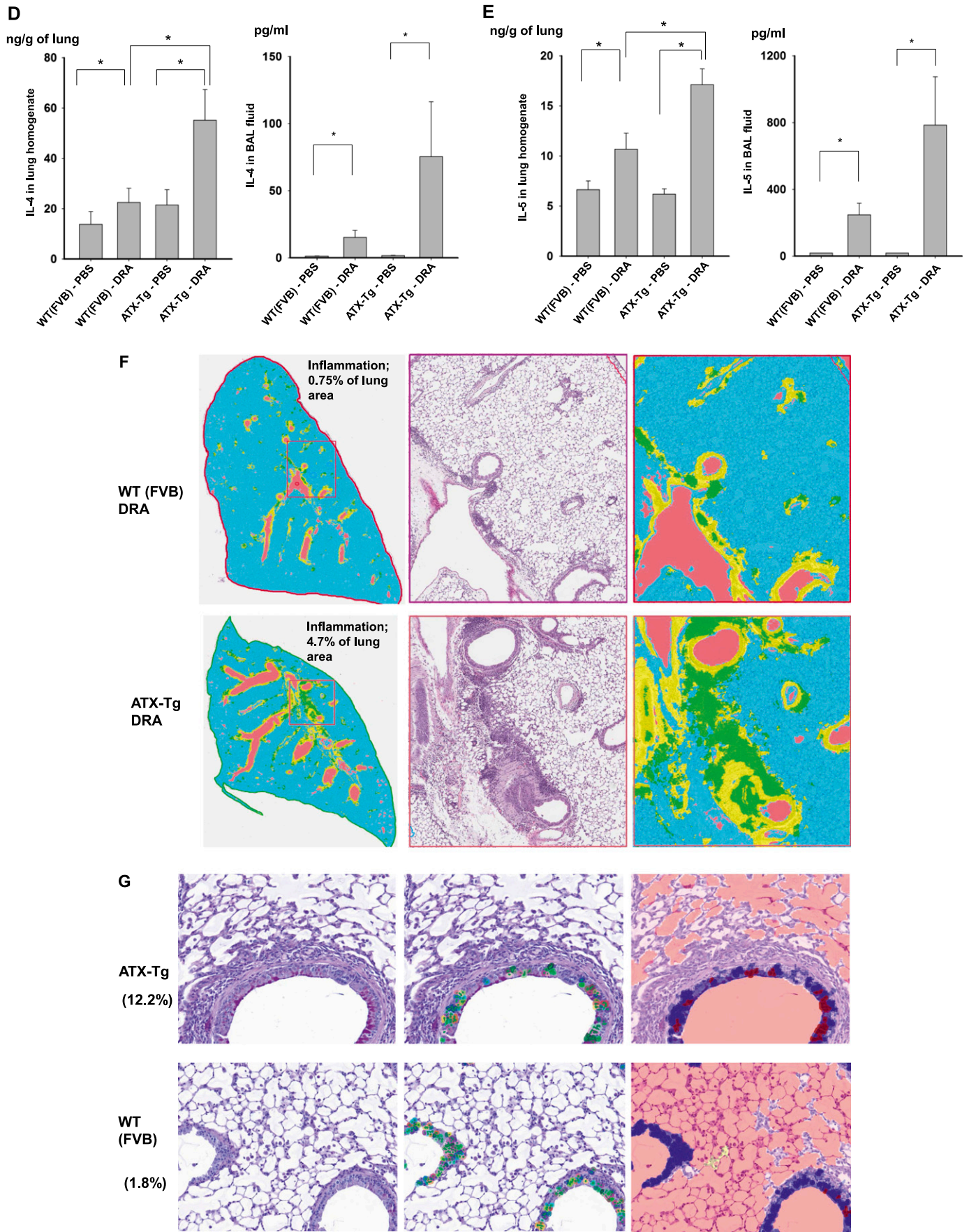


Figure 3. (continued).

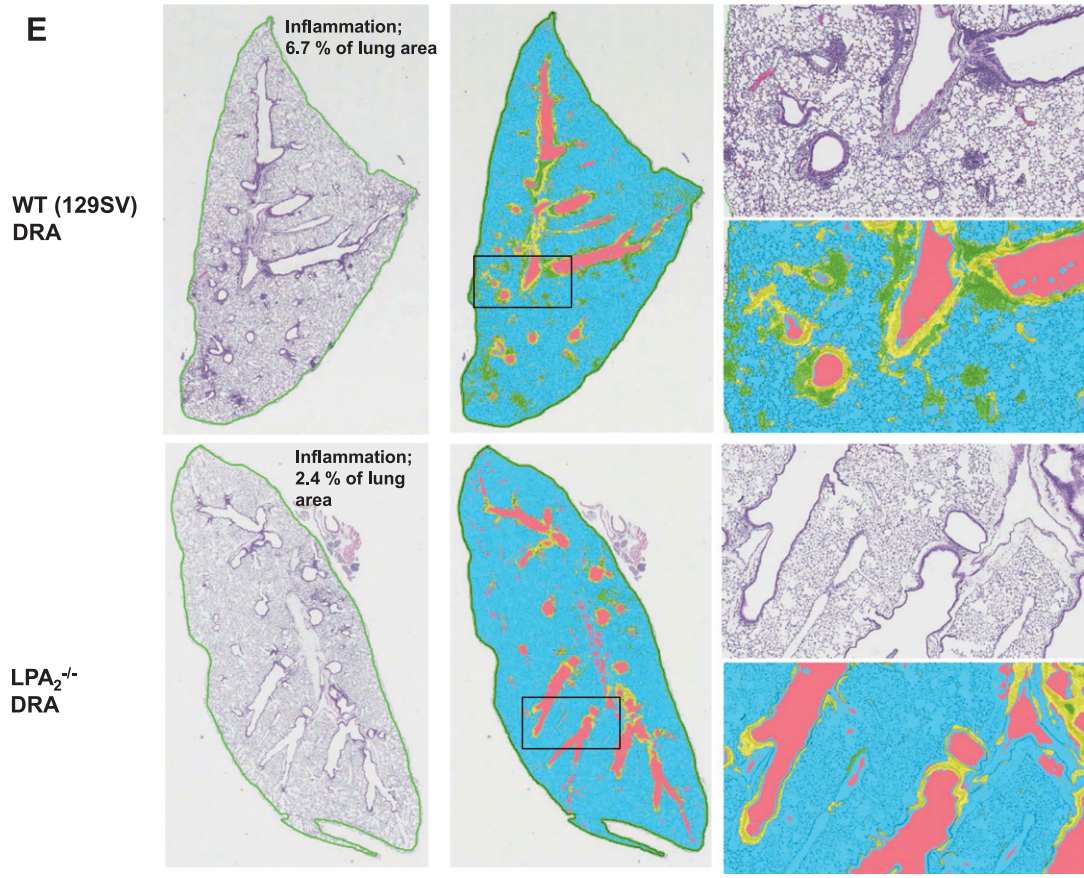
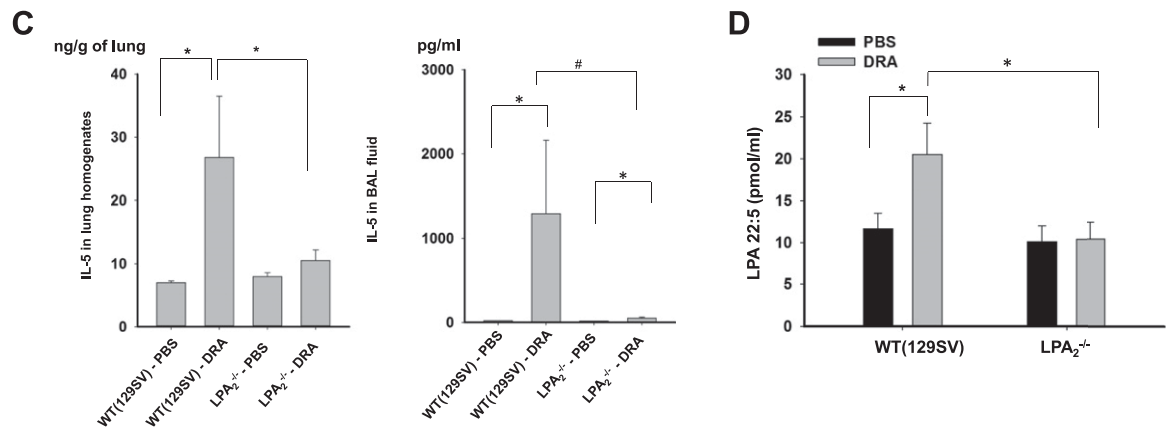
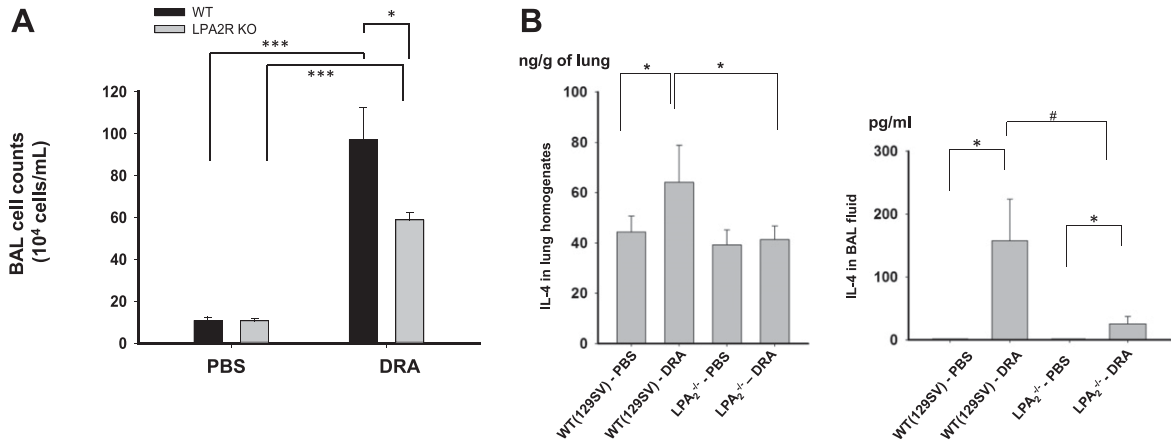


Figure 4. (A) Total cell counts in bronchoalveolar lavage (BAL) fluid of wild-type (WT) versus lysophosphatidic acid (LPA)₂^{-/-} knock-out (KO) mice induced by the house dust mite, ragweed, *Aspergillus* sp. (DRA) triple-allergen model. LPA₂^{-/-} mice had lower numbers of total cells in BAL fluid after allergen challenge compared with WT mice of the same background (WT-129SV). $n \geq 5$ mice per group. * $P < 0.05$; *** $P < 0.001$. (B) Concentration of IL-4 in whole lung homogenates and BAL fluids of the LPA₂^{-/-} versus WT-129SV mice induced by the DRA triple-allergen model. Experiments were done at least twice with similar results. $n \geq 5$ mice per group. * $P < 0.05$; # $P = 0.10$. (C) Concentration of IL-5 in whole lung homogenates and BAL fluids of LPA₂^{-/-} versus WT-129SV mice induced by DRA triple-allergen model. Experiments were done at least twice with similar results. $n \geq 5$ mice per group. * $P < 0.05$; # $P = 0.055$. (D) Level of LPA 22:5 in BAL fluids from LPA₂^{-/-} versus WT-129SV mice induced in the DRA triple-allergen model. LPA levels were measured by liquid chromatography with tandem mass spectrometry as described in METHODS. * $P < 0.05$; $n = 9$. (E) Pathologic severity of allergic lung inflammation in LPA₂^{-/-} versus WT-129SV mice in the DRA triple-allergen model. The whole lung field was scanned and analyzed as described in METHODS. The numeric values represent the percentage of regional area of lung inflammation. The analysis was repeated at least twice with similar results. The color codes represent the following: *green* = inflammation, *blue* = alveolar space, *yellow* = structural tissue, and *pink* = void area. PBS = phosphate-buffered saline.

temperature equal to 1 hour (Figure E16). Quantification of lung pathology also showed reduced inflammation with ATX inhibitor treatment (Figure 5D). These results indicate that the ATX/LPA axis is necessary for the generation of asthmatic inflammation and may be an important new target for therapeutic intervention in severe asthma.

DISCUSSION

Asthma is a heterogeneous allergic airway inflammatory disease of unknown etiology that is believed to result from a combination of environmental exposure and genetic susceptibility. Many pathogenic mechanisms of asthma have been proposed, but few have been successfully translated into effective treatments. The pathophysiology of asthma involves various cellular components and many inflammatory protein mediators, including chemokines, cytokines, growth factors, and various lipid mediators (24). Bioactive lipid mediators such as cysteinyl leukotrienes and prostaglandins are believed to play an important role in asthma pathophysiology, and interdiction with leukotriene receptor antagonists is an effective and widely used treatment that alleviates symptoms in some patients with asthma (25). Recent evidence suggests that prostaglandin D2 may play an important role in orchestrating interaction between mast cells, lymphocytes, and eosinophils (26), and this finding is currently being translated into antiasthmatic therapeutics with some initial evidence of efficacy (27).

Here, we report that a novel bioactive lipid mediator, LPA, has a pivotal role in the pathogenesis of asthma through studies exploring a model of human asthmatic lung inflammation and a triple-allergen-induced model of lung inflammation in genetically modified mice. LPA is synthesized from LPC through the enzymatic activity of ATX (2). Our clinical data show that the levels of ATX protein, and very specific polyunsaturated molecular species of the enzymatic products of ATX, LPA 22:5 and 22:6, are significantly elevated in the airspaces of patients with mild asthma in response to subsegmental bronchial allergen challenge in both a discovery and verification cohort of volunteers. LPA22:5 and LPA 22:6 are rare LPA molecular species in biologic fluids. Because of an exceptionally long acyl chain, LPA22:6, and probably LPA 22:5, are folded into the enzymatic pocket of ATX in a unique U-shaped conformation (28). Our result showed that LPA 22:5 and 22:6 in the BAL fluids were elevated 11- and 7-fold, respectively, in response to allergen challenge (Figures 2B–2D). It is highly unlikely that these LPA species are derived from plasma leak into the airspaces, because there was no increase in the plasma level of LPA 22:5 and 22:6 induced by subsegmental challenge. Furthermore, the saturated fatty acid profile of plasma LPA species induced by allergen challenge was completely different from that of the

BAL fluid (Figure 2F). It is unclear how these two different LPA profiles are generated in the blood and airspace compartments by allergen challenge, but differences in the bioavailability of saturated versus polyunsaturated LPC substrates and/or the presence of different ATX isoenzymes may contribute to the dichotomy. Interestingly, the ATX/LPA pathway has been proposed as a homeostatic mechanism for lymphocyte trafficking. There is growing evidence that the expression of ATX on high-endothelial venules (HEVs) of secondary lymphoid tissues and its metabolic products of LPA play an important role in lymphocyte trafficking across HEVs (29, 30). LPA with 18:0, 18:1, and 18:2 long-chain fatty acids are important LPA molecular species produced by HEVs and play a role in systemic lymphocyte trafficking (30). However, in the case of locally induced inflammation models used in our current experiments, LPA 22:5 and 22:6 are likely important for the local proallergic reaction, which could be negatively counterbalanced by systemic production of LPA 16:0 and 18:0 that would promote lymphocyte homing and confine the allergic reaction to the locally challenged site. Of note, similar to previously reported asthma phenotypes (31), we also observed a heterogeneity in the ATX-LPA responsiveness of our asthma cohorts; some subjects showed a more blunted increase in their allergen challenge-induced LPA response in BAL fluid, although the overall responsiveness was statistically significant by paired *t* test (Figure 2D).

Ovalbumin has been widely used in animal models of allergic lung inflammation, but it is not a clinically relevant allergen for human asthma. Because house dust mite and ragweed were the major aeroallergens used for our human SBP-AG protocol in patients with mild asthma, we used these as well in the murine triple-allergen (DRA) allergic asthma model, instead of ovalbumin. By using the DRA murine asthma model, we were highly successful in recapitulating the findings from human asthmatic SBP-AG subjects in mice. Additionally, we confirmed that a gain-of-function increase in ATX expression in mice accentuates the asthma phenotype in terms of Th2 cytokine production and allergic lung inflammation. We also demonstrate that the combined genetic (partial ATX gene knockout) and pharmacologic (ATX enzyme inhibitor) inhibition of the ATX-LPA pathway significantly attenuates the development of both Th2 immunologic responses and inflammatory reactions in the mouse DRA model. Of note, mice lacking the LPA₂ receptor were resistant to the development of asthmatic lung inflammation in this model. LPA₂, a member of the LPA receptor family, is a G-protein-coupled transmembrane receptor. LPA₂ has been shown to promote cell migration through interactions with the focal adhesion molecule TRIP6 (32), and zinc finger proteins are also reported to interact directly with the carboxyl terminal tail of LPA₂ (33), suggesting LPA₂ signaling has cross-regulation between classical G-protein signaling and other pathways to

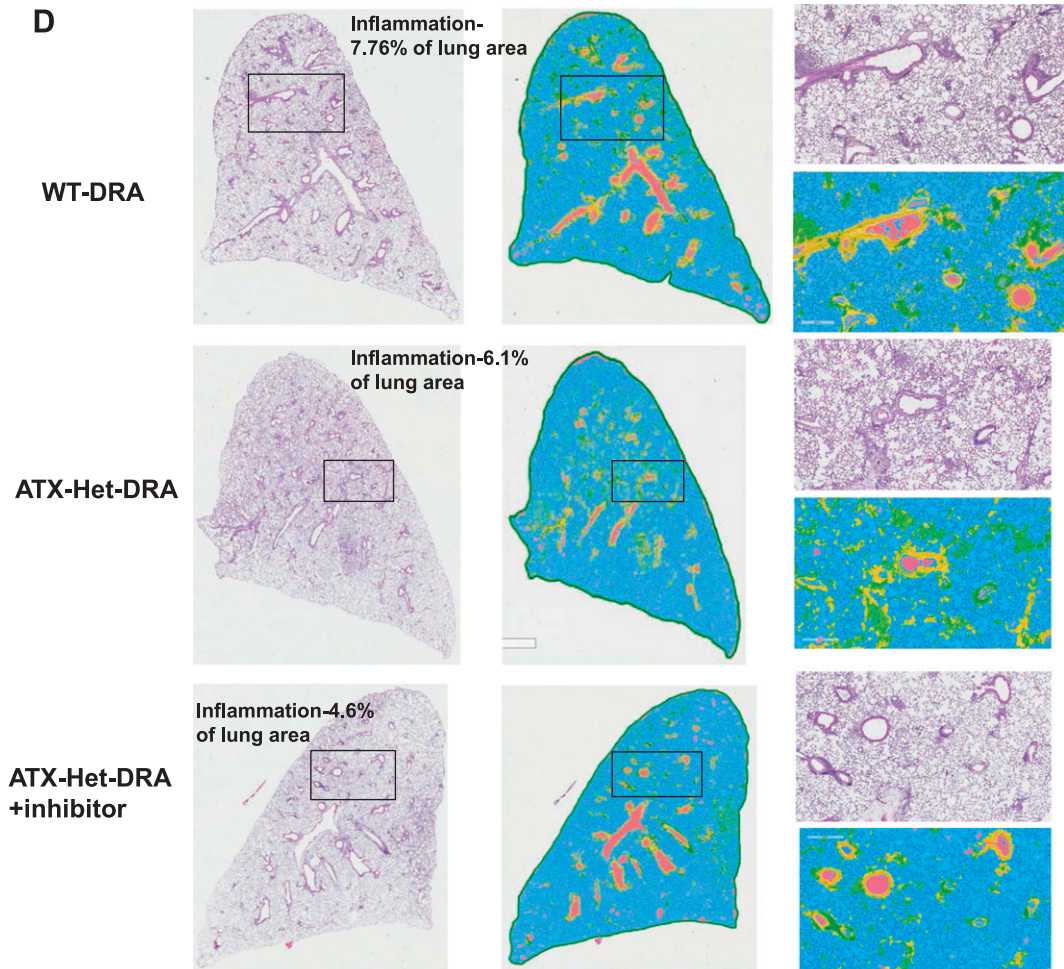
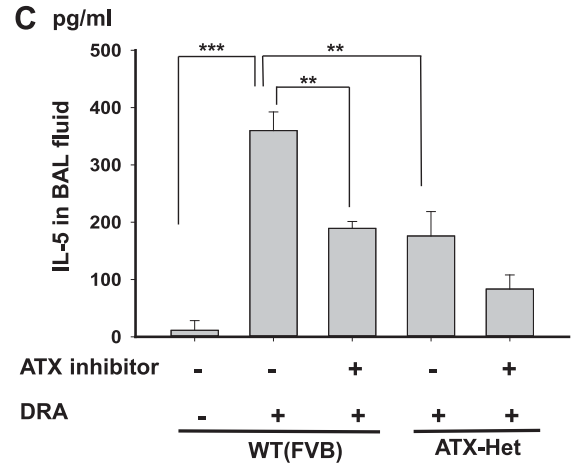
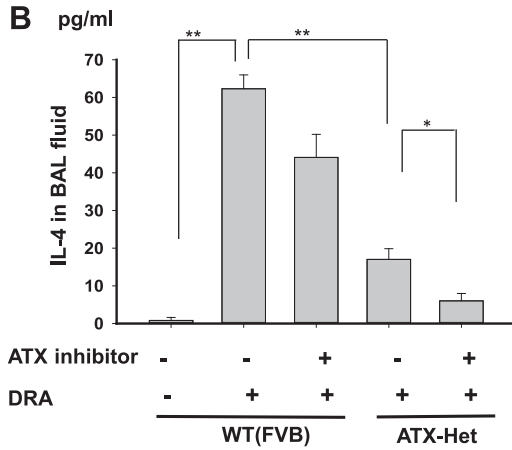
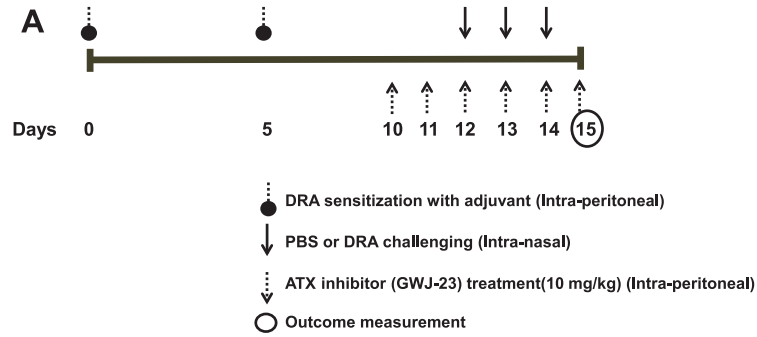


Figure 5. (A) Diagram of the experimental design used for the autotaxin (ATX) inhibitor, GWJ-23, in wild-type (WT) and ATX-heterozygous (ATX-het) mice in the house dust mite, ragweed, *Aspergillus* sp. (DRA) triple-allergen model. All mice had received either GWJ (ATX inhibitor) or equivalent dose of the vehicle (dimethyl sulfoxide). (B) Concentration of IL-4 in bronchoalveolar lavage (BAL) fluids of ATX-het versus WT mice induced in the DRA triple-allergen model. ATX-het and WT mice were sensitized and challenged in the DRA model, with and without treatment using an ATX enzyme inhibitor (GWJ-23). The ATX inhibitor was administered intranasally multiple times after allergen sensitization but before intranasal challenge with the DRA allergens, as described in detail in A. $n \geq 5$ mice per group. $*P < 0.05$; $**P < 0.01$. (C) Concentration of IL-5 in BAL fluids of ATX-het versus WT mice induced in the DRA triple-allergen model. ATX-het and WT mice were interrogated using the DRA model with and without treatment with the ATX inhibitor, GWJ-23. The ATX inhibitor was administered intranasally at multiple times before intranasal challenge with the DRA allergens, as described in A. $n \geq 5$ mice per group. $**P < 0.01$; $***P < 0.001$. (D) Pathologic severity of allergic lung inflammation in WT, ATX-Het mice, and ATX-Het with ATX inhibitor treatment in the DRA triple-allergen model. The numeric values represent the percentage of regional area of lung inflammation. The analysis was repeated at least twice, with similar results. PBS = phosphate-buffered saline.

regulate the efficiency and specificity of signal transduction (21). In contrast to our current findings and an earlier report on LPA₂ and allergic airway inflammation (34), a previous study showed that LPA₂ deficiency negatively regulated dendritic cell activation and allergic inflammation in a murine model of asthma (35). The reasons for this discrepancy are unclear, but may be related to the nature of the allergens used for sensitization and challenge and the genetic backgrounds of the mice.

There are some limitations to our current study. In the allergic airspace, ATX produced unique LPA molecular species, LPA 22:5 and LPA 22:6, but we have yet to determine the cell source of the enzymatic substrate, polyunsaturated LPC, for their generation. Although our data suggest alveolar macrophages as a source of ATX, the contribution of other cell types, including airway epithelial cells, which are rich in polyunsaturated phospholipids (36) and eosinophils, cannot be excluded. The recently reported crystal structure of ATX revealed that the somatomedin B (SMB) domains of ATX are homologous to the SMB domain of vitronectin, whose RGD motif binds integrins (37). It has been proposed that the interaction between integrin and SMB domain of ATX enables localized production of LPA in the area of activated integrins expression. The interaction of both platelet $\beta 1$ and $\beta 3$ integrins with ATX via the SMB2 domain in an activation-dependent manner has been reported (38). Recruitment of eosinophils into sites of local allergic inflammation requires the expression of integrins, including $\beta 1$ (39). It would be of interest to determine whether integrins expressed on eosinophils interact with ATX, which could then act on its own receptors. Although the biological response to LPA is mediated in part through binding to the LPA₂ receptor in the murine allergic asthma model, which may be present on eosinophils, T lymphocytes, and airway smooth muscle cells, the participating LPA receptors on human inflammatory and airway cells has not been determined. Finally, future studies that address the direct effects of polyunsaturated LPA 22:5 and LPA 22:6 on the experimental asthma phenotype are needed to fully interrogate their potentially selective role in ATX/LPA signaling before our pre-clinical findings can be translated into the development of novel antiasthmatic therapeutics.

Author disclosures are available with the text of this article at www.atsjournals.org.

Acknowledgment: The authors thank all of the generous subjects with asthma who volunteered for the SBP-AG protocol. They also thank the entire staff of the Clinical Interface Core at the University of Illinois Center for Clinical and Translational Science (UIC-CCTS) for assistance with patient recruitment, screening, and performing bronchoscopy. They also thank Minghui (Norma) Xing, Fan (Kimberly) Gao, and Preeth Alumkal for technical assistance in the inflammatory cell purification core, and Loren Denlinger and Elizabeth Schwantes at the University of Wisconsin for training in SBP-AG bronchoscopy procedure and inflammatory cell purification protocols, Min-Jong Kang and Chun Geun Lee at Yale University for training on the mouse asthma model, and James J. Lee at Mayo Clinic Arizona for provision of anti-mouse MBP1 antibody.

References

1. Tokumura A. Physiological and pathophysiological roles of lysophosphatidic acids produced by secretory lysophospholipase D in body fluids. *Biochim Biophys Acta* 2002;1582:18–25.
2. Tokumura A, Majima E, Kariya Y, Tominaga K, Kogure K, Yasuda K, Fukuzawa K. Identification of human plasma lysophospholipase D, a lysophosphatidic acid-producing enzyme, as autotaxin, a multifunctional phosphodiesterase. *J Biol Chem* 2002;277:39436–39442.
3. Kranenburg O, Poland M, van Horck FPG, Drechsel D, Hall A, Moolenaar WH. Activation of RhoA by lysophosphatidic acid and $\alpha 12/13$ subunits in neuronal cells: induction of neurite retraction. *Mol Biol Cell* 1999;10:1851–1857.
4. Wang L, Cummings R, Zhao Y, Kazlauskas A, Sham JKS, Morris A, Georas S, Brindley DN, Natarajan V. Involvement of phospholipase D2 in lysophosphatidate-induced transactivation of platelet-derived growth factor receptor- β in human bronchial epithelial cells. *J Biol Chem* 2003;278:39931–39940.
5. Ediger TL, Danforth BL, Toews ML. Lysophosphatidic acid upregulates the epidermal growth factor receptor in human airway smooth muscle cells. *Am J Physiol Lung Cell Mol Physiol* 2002;282:L91–L98.
6. Hashimoto T, Yamashita M, Ohata H, Momose K. Lysophosphatidic acid enhances in vivo infiltration and activation of guinea pig eosinophils and neutrophils via a Rho/Rho-associated protein kinase-mediated pathway. *J Pharmacol Sci* 2003;91:8–14.
7. Zhao Y, He D, Zhao J, Wang L, Leff AR, Spannhake EW, Georas S, Natarajan V. Lysophosphatidic acid induces interleukin-13 (IL-13) receptor alpha2 expression and inhibits IL-13 signaling in primary human bronchial epithelial cells. *J Biol Chem* 2007;282:10172–10179.
8. Saatian B, Zhao Y, He D, Georas SN, Watkins T, Spannhake EW, Natarajan V. Transcriptional regulation of lysophosphatidic acid-induced interleukin-8 expression and secretion by p38 MAPK and JNK in human bronchial epithelial cells. *Biochem J* 2006;393:657–668.
9. Rubinfeld J, Guo J, Sookrung N, Chen R, Chaicumpa W, Casolaro V, Zhao Y, Natarajan V, Georas S. Lysophosphatidic acid enhances interleukin-13 gene expression and promoter activity in T cells. *Am J Physiol Lung Cell Mol Physiol* 2006;290:L66–L74.
10. Toews ML, Ustinova EE, Schultz HD. Lysophosphatidic acid enhances contractility of isolated airway smooth muscle. *J Appl Physiol* 1997; 83:1216–1222.
11. Zhao Y, Natarajan V. Lysophosphatidic acid signaling in airway epithelium: role in airway inflammation and remodeling. *Cell Signal* 2009;21: 367–377.
12. Ediger TL, Toews ML. Synergistic stimulation of airway smooth muscle cell mitogenesis. *J Pharmacol Exp Ther* 2000;294:1076–1082.
13. Wang L, Knudsen E, Jin Y, Gessani S, Maghazachi AA. Lysophospholipids and chemokines activate distinct signal transduction pathways in T helper 1 and T helper 2 cells. *Cell Signal* 2004;16:991–1000.
14. Idzko M, Laut M, Panther E, Soricther S, Durk T, Fluhr JW, Herouy Y, Mockenhaupt M, Myrtek D, Elsner P, *et al.* Lysophosphatidic acid induces chemotaxis, oxygen radical production, CD11B up-regulation, Ca²⁺ mobilization, and actin reorganization in human eosinophils via pertussis toxin-sensitive G proteins. *J Immunol* 2004;172:4480–4485.
15. Georas SN, Berdyshev E, Hubbard W, Gorchkova IA, Usatyuk PV, Saatian B, Myers AC, Williams MA, Xiao HQ, Liu M, *et al.* Lysophosphatidic acid is detectable in human bronchoalveolar lavage fluids at baseline and increased after segmental allergen challenge. *Clin Exp Allergy* 2007;37:311–322.

16. Tager AM, LaCamera P, Shea BS, Campanella GS, Selman M, Zhao Z, Polosukhin V, Wain J, Karimi-Shah BA, Kim ND, *et al.* The lysophosphatidic acid receptor LPA1 links pulmonary fibrosis to lung injury by mediating fibroblast recruitment and vascular leak. *Nat Med* 2008;14:45–54.
17. Pamuklar Z, Federico L, Liu S, Umezu-Goto M, Dong A, Panchatcharam M, Fulerson Z, Berdyshev E, Natarajan V, Fang X, *et al.* Autotaxin/lysopholipase D and lysophosphatidic acid regulate murine hemostasis and thrombosis. *J Biol Chem* 2009;284:7385–7394.
18. Contos JJA, Ishii I, Fukushima N, Kingsbury MA, Ye X, Kawamura S, Brown JH, Chun J. Characterization of lpa2 (Edg4) and lpa1/lpa2 (Edg2/Edg4) lysophosphatidic acid receptor knockout mice: signaling deficits without obvious phenotypic abnormality attributable to lpa2. *Mol Cell Biol* 2002;22:6921–6929.
19. Goplen N, Karim MZ, Liang Q, Gorska MM, Rozario S, Guo L, Alam R. Combined sensitization of mice to extracts of dust mite, ragweed, and *Aspergillus* species breaks through tolerance and establishes chronic features of asthma. *J Allergy Clin Immunol* 2009;123:925–932.e11.
20. Zhao J, He D, Su Y, Berdyshev E, Chun J, Natarajan V, Zhao Y. Lysophosphatidic acid receptor 1 modulates lipopolysaccharide-induced inflammation in alveolar epithelial cells and murine lungs. *Am J Physiol Lung Cell Mol Physiol* 2011;301:L547–L556.
21. Choi JW, Herr DR, Noguchi K, Yung YC, Lee CW, Mutoh T, Lin ME, Teo ST, Park KE, Mosley AN, *et al.* LPA receptors: subtypes and biological actions. *Annu Rev Pharmacol Toxicol* 2010;50:157–186.
22. Oikonomou N, Mouratis M-A, Tzouveleki A, Kaffe E, Valavanis C, Vilaras G, Karameris A, Prestwich GD, Bouros D, Aidinis V. Pulmonary autotaxin expression contributes to the pathogenesis of pulmonary fibrosis. *Am J Respir Cell Mol Biol* 2012;47:566–574.
23. Jiang G, Madan D, Prestwich GD. Aromatic phosphonates inhibit the lysophospholipase D activity of autotaxin. *Bioorg Med Chem Lett* 2011;21:5098–5101.
24. Barnes PJ. The cytokine network in asthma and chronic obstructive pulmonary disease. *J Clin Invest* 2008;118:3546–3556.
25. Nagai H. Recent research and developmental strategy of anti-asthma drugs. *Pharmacol Ther* 2012;133:70–78.
26. Lilly CM, Palmer LJ. The role of prostaglandin D receptor gene in asthma pathogenesis. *Am J Respir Cell Mol Biol* 2005;33:224–226.
27. Barnes N, Pavord I, Chuchalin A, Bell J, Hunter M, Lewis T, Parker D, Payton M, Collins LP, Pettipher R, *et al.* A randomized, double-blind, placebo-controlled study of the CRTH2 antagonist OC000459 in moderate persistent asthma. *Clin Exp Allergy* 2012;42:38–48.
28. Nishimasu H, Ishitani R, Aoki J, Nureki O. A 3D view of autotaxin. *Trends Pharmacol Sci* 2012;33:138–145.
29. Bai Z, Cai L, Umemoto E, Takeda A, Tohya K, Komai Y, Veeraveedu PT, Hata E, Sugiura Y, Kubo A, *et al.* Constitutive lymphocyte transmigration across the basal lamina of high endothelial venules is regulated by the autotaxin/lysophosphatidic acid axis. *J Immunol* 2013;190:2036–2048.
30. Zhang Y, Chen Y-CM, Krummel MF, Rosen SD. Autotaxin through lysophosphatidic acid stimulates polarization, motility, and transendothelial migration of naive T cells. *J Immunol* 2012;189:3914–3924.
31. Wenzel S. Severe asthma: from characteristics to phenotypes to endotypes. *Clin Exp Allergy* 2012;42:650–658.
32. Lai Y-J, Chen C-S, Lin W-C, Lin F-T. c-Src-mediated phosphorylation of TRIP6 regulates its function in lysophosphatidic acid-induced cell migration. *Mol Cell Biol* 2005;25:5859–5868.
33. Lin FT, Lai YJ. Regulation of the LPA2 receptor signaling through the carboxyl-terminal tail-mediated protein–protein interactions. *Biochim Biophys Acta* 2008;1781:558–562.
34. Zhao Y, Tong J, He D, Pendyala S, Evgeny B, Chun J, Sperling AI, Natarajan V. Role of lysophosphatidic acid receptor LPA2 in the development of allergic airway inflammation in a murine model of asthma. *Respir Res* 2009;10:114.
35. Emo J, Meednu N, Chapman TJ, Rezaee F, Balys M, Randall T, Rangasamy T, Georas SN. LPA2 is a negative regulator of both dendritic cell activation and murine models of allergic lung inflammation. *J Immunol* 2012;188:3784–3790.
36. Berry KA, Li B, Reynolds SD, Barkley RM, Gijon MA, Hankin JA, Henson PM, Murphy RC. Maldit imaging MS of phospholipids in the mouse lung. *J Lipid Res* 2011;52:1551–1560.
37. Hausmann J, Kamtekar S, Christodoulou E, Day JE, Wu T, Fulkerson Z, Albers HMHG, van Meeteren LA, Houben AJS, van Zeijl L, *et al.* Structural basis of substrate discrimination and integrin binding by autotaxin. *Nat Struct Mol Biol* 2011;18:198–204.
38. Fulkerson Z, Wu T, Sunkara M, Kooi CV, Morris AJ, Smyth SS. Binding of autotaxin to integrins localizes lysophosphatidic acid production to platelets and mammalian cells. *J Biol Chem* 2011;286:34654–34663.
39. Barthel SR, Johansson MW, McNamee DM, Mosher DF. Roles of integrin activation in eosinophil function and the eosinophilic inflammation of asthma. *J Leukoc Biol* 2008;83:1–12.